Jonathan H. Burdette, MD
Allen D. Elster, MD
Peter E. Ricci, MD

Index terms:
Brain, infarction, 10.78
Brain, MR, 10.12144
Magnetic resonance (MR), diffusion study, 10.12144

Radiology 1999; 212:333–339

Abbreviations:
ADC = apparent diffusion coefficient
DW = diffusion weighted
SI = signal intensity

[1] From the Department of Radiology, Wake Forest University School of Medicine, the Bowman Gray Campus, Medical Center Blvd, Winston-Salem, NC 27157. From the 1998 RSNA scientific assembly. Received August 26, 1998; revision requested November 2; revision received November 30; accepted March 1, 1999. Supported in part by a grant from GE Medical Systems. **Address reprint requests to** J.H.B. (e-mail: *jburdett@rad.wfubmc.edu*).

Author contributions:
Guarantor of integrity of entire study, J.H.B.; study concepts and design, A.D.E., J.H.B., P.E.R.; definition of intellectual content, J.H.B., A.D.E., P.E.R.; literature research, J.H.B., A.D.E., P.E.R.; clinical studies, J.H.B., P.E.R., A.D.E.; data acquisition, J.H.B.; data analysis, J.H.B., P.E.R., A.D.E.; statistical analysis, J.H.B., A.D.E.; manuscript preparation, J.H.B., A.D.E.; manuscript editing and review, J.H.B., A.D.E., P.E.R.

Acute Cerebral Infarction: Quantification of Spin-Density and T2 Shine-through Phenomena on Diffusion-weighted MR Images[1]

PURPOSE: To quantify the relative contributions of spin density and T2 effects (''shine through'') on diffusion-weighted (DW) magnetic resonance (MR) images of acute and subacute cerebral infarction.

MATERIALS AND METHODS: In 30 patients, 1.5-T imaging was performed within the first 7 days after onset of cerebral infarction. Estimates of T2, spin density, and apparent diffusion coefficient (ADC) in the region of stroke and contralateral normal brain were computed by means of standard regression techniques after quadruple-echo conventional MR imaging and single-shot echo-planar DW imaging with a maximum *b* value of 1,000 sec/mm^2. Expected signal intensity (SI) enhancement ratios resulting from independent changes in T2, spin density, and ADC were then calculated for the DW sequence.

RESULTS: The overall SI of cerebral infarction on DW images was significantly higher than that of normal brain throughout the 1st week after stroke (mean relative SI enhancement ratio, 2.29; $P < .001$). During the first 2 days after stroke, decreased ADC within the stroke region made the dominant contribution to increased SI on DW images. By day 3, increased T2 values in the stroke region became equally important, and, from days 3–7, the contribution to SI from T2 effects became dominant. A slight increase of spin density in the stroke region made a relatively small and constant contribution to DW SI over the 1st week.

CONCLUSION: The increased SI of subacute cerebral infarction on DW images reflects not only a shortening of ADC but a prolongation of T2 and spin-density values.

The utility of diffusion-weighted (DW) magnetic resonance (MR) imaging for the diagnosis of acute cerebral infarction has now been thoroughly established (1–19). DW imaging is a relatively new technique that uses powerful imaging gradients coupled with rapid spin-echo or echo-planar data acquisition to accentuate phase differences between protons of varying mobility. In regions of recent cerebral infarction, the diffusion of tissue water becomes restricted, as manifested by a decrease in its apparent diffusion coefficient (ADC).

Alterations in brain diffusion by disease can be represented in an anatomically meaningful format by using either of two methods: (*a*) display of a DW image, in which the brightness of each pixel is proportional to the magnitude of the MR signal intensity (SI) recorded under maximum strength application of the diffusion-sensitizing gradient, or (*b*) display of an ADC map, in which the brightness of each pixel is proportional to its calculated ADC value.

The diagnostic information provided by DW images and ADC maps is not identical. For example, the time course of SI changes after an acute infarction differs markedly depending on the display method employed (8,11,13,14,16,17). Specifically, ADC maps typically

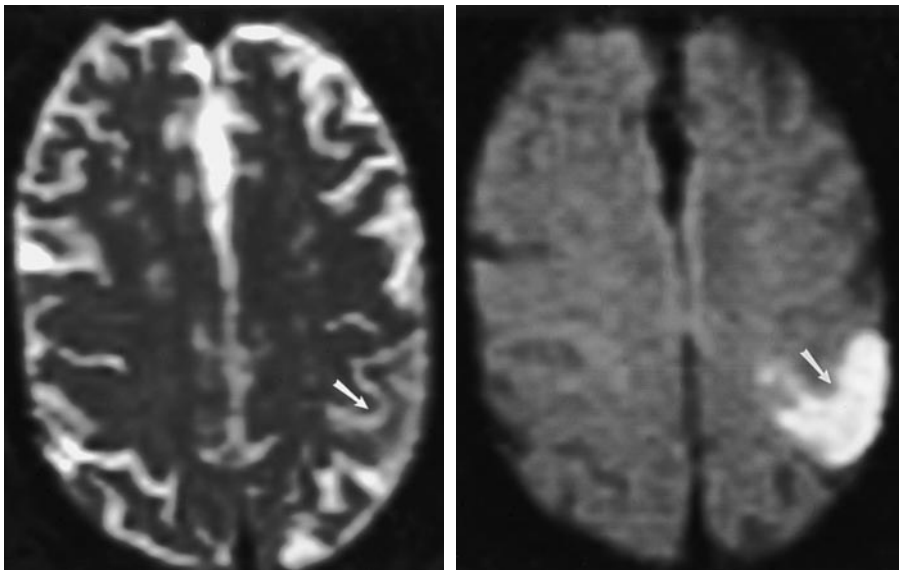

a. **b.**

Figure 1. Case 5. Echo-planar MR images in a 71-year-old man with a 36-hour-old cerebral infarction in the left anterior parietal region. **(a)** On the T2-weighted image (10,000/97 with *b* value of 1 sec/mm^2), the infarct (arrow) is extremely subtle. **(b)** However, on the DW image (10,000/97 with *b* value of 1,000 sec/mm^2), the infarct (arrow) is very conspicuous. When the infarct is compared with normal contralateral brain, there is only a 7% increase in the T2 value within the infarct, whereas there is a 55% decrease in ADC value. Thus, almost all of the abnormal increased SI in **b** arises from diffusion effects.

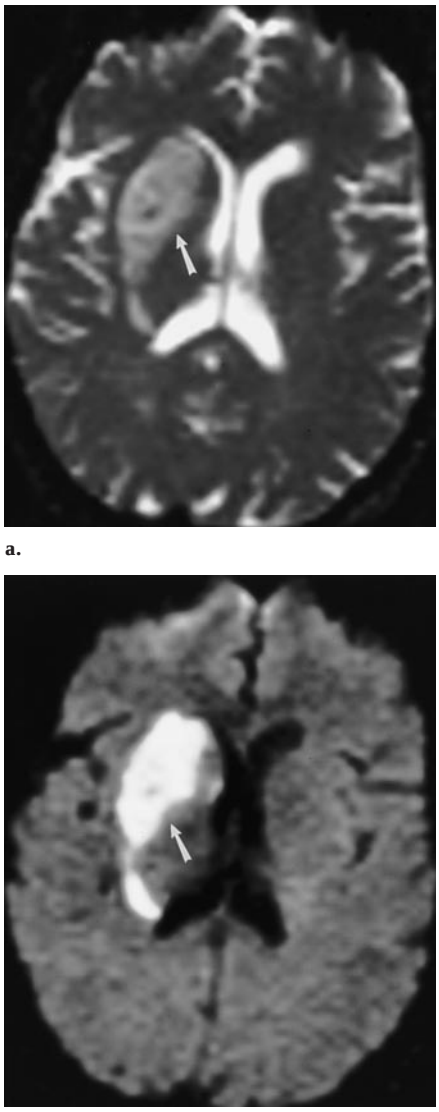

a. **b.**

Figure 2. Case 18. Echo-planar MR images in an 80-year-old man with a 4-day-old cerebral infarction in the right basal ganglia (arrow). The infarct is apparent on both the **(a)** T2-weighted image (10,000/97 with *b* value of 1 sec/mm^2) and **(b)** DW image (10,000/97 with *b* value of 1,000 sec/mm^2). With a T2 increase of 36%, ADC decrease of 33%, and spin-density increase of 38% within the infarct, there is similar contribution to the increased SI within the infarct in **b** from each parameter.

return to normal within 7–10 days after stroke, whereas DW images may remain abnormal for up to 14 days (14).

Just as a so-called T2-weighted image is not a simple map of T2 values, a DW image is not a simple map of diffusion constants. Rather, DW images contain mixed contributions from changes in T2, spin density, and ADC. We refer to these spillover effects of T2 and spin density on the DW image as MR "shine through." The purpose of this study was to quantify MR shine-through effects in the DW imaging of acute and subacute cerebral infarction.

MATERIALS AND METHODS

Our study population comprised 30 patients (16 male and 14 female patients; age range, 4–84 years; mean age, 64 years). All had been referred for MR imaging from March 1998 through June 1998 with definitive clinical evidence of a cerebral infarction less than 7 days old. A reliable time of clinical ictus could be established in all patients to within plus or minus 6 hours, as determined by means of review of the medical records, consultation with the referring physician, and/or direct patient interview. Ten patients underwent imaging during the first 48 hours after clinical stroke, 12 patients between 48 and 96 hours, and eight patients between 4.5 and 7 days.

MR imaging was performed in all subjects with a commercially available echo-planar instrument operating at 1.5 T (Signa EchoSpeed Horizon; GE Medical Systems, Milwaukee, Wis). Conventional axial spin-echo MR images were obtained with a multiecho technique, with a repetition time of 4,000 msec and echo times of 40, 80, 120, and 160 msec (4,000/40, 80, 120, 160). Other imaging parameters included one signal acquired, field of view of 24 cm, acquisition matrix of 256 × 128, and section thickness of 5 mm with a 2.5-mm intersection gap. A single-shot echo-planar DW imaging sequence was then performed with the following parameters: 10,000/97, one signal acquired, field of view of 30 cm, acquisition matrix of 128 × 128, and section thickness of 5 mm with a 2.5-mm intersection gap. Diffusion gradients were sequentially activated in each of the three principal anatomic axes to obtain DW images sensitive to diffusion in the x, y, and z planes. Gradient strengths corresponding to *b* values of 1 and 1,000 sec/mm^2 were used. This commercially available diffusion imaging software produced 20 axial images, covering the entire brain in 40 seconds.

For the two *b* value image sets and the quadruple echo time image sets, region-of-interest SIs were obtained in the core of the cerebral infarction and within normal contralateral brain by a neuroradiologist (J.H.B.). Within the infarct and normal brain for each patient, the size and location of the region of interest remained constant (ie, maintained the same size for the two *b* value image sets and the quadruple echo time image sets). The trace value of the estimated diffusion tensor

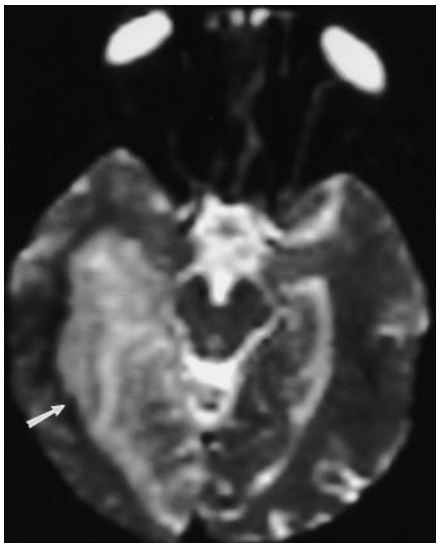

a.

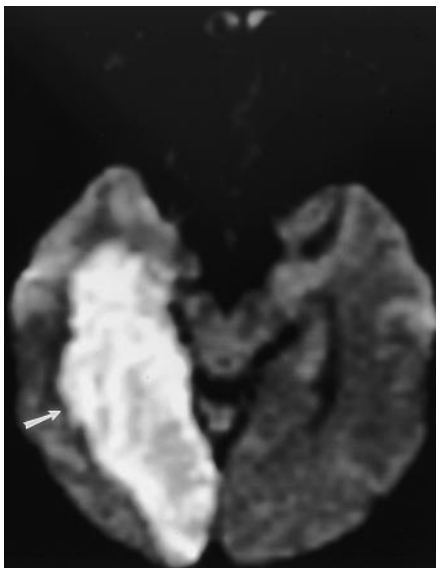

b.

Figure 3. Case 29. Echo-planar MR images in a 60-year-old man with a 7-day-old cerebral infarction (arrow) in the right occipital and medial temporal lobes. The infarct is apparent on both the **(a)** T2-weighted (10,000/97 with *b* value of 1 sec/mm^2) and **(b)** DW (10,000/97 with *b* value 1,000 sec/mm^2) images. These images show the decreasing contribution of ADC and increasing contribution of T2 effects to SI within infarcts on DW images with increasing time. In this case, there was an increase in T2 of 58%, ADC decrease of 26%, and spin density increase of 38% within the infarct, indicating dominance of the T2 effects in **b**.

was used for each ADC measurement, representing the average of region-of-interest values along the three principal diffusion axes.

The data were analyzed by means of standard linear and nonlinear regression models by using commercially available statistical software (Systat, Evanston, Ill). Calculations of ADC values were obtained for infarct and normal brain by applying the Stejskal-Tanner equation (20) with two *b* values of 1 and 1,000 sec/mm^2. This two-point estimation of ADC values has recently been shown to be highly accurate by two independent groups of investigators (21,22). Estimates of T2 and relative spin density were obtained by using measurements from the long repetition time, quadruple echo time sequence. These estimates were obtained by means of nonlinear parameter fitting to the well-recognized formula for spin-echo SI derived from the Bloch equations (23,24). For each patient, therefore, six estimated tissue parameters were calculated: three in the region of stroke (spin density [SD_S], $T2_S$, and ADC_S) and three in normal brain contralateral to the stroke (SD_N, $T2_N$, and ADC_N).

TABLE 1
Tissue Parameters Measured in Normal Brain and the Stroke Region

Parameter	Normal Brain	Stroke Region
Spin density (relative units)	0.88 ± 0.13	1.07 ± 0.20
T2 (msec)	85 ± 12	120 ± 17
ADC ($\times 10^{-4}$ mm^2/sec)	7.9 ± 1.1	5.1 ± 1.2

Note.—Numbers are the mean ± SD (n = 30). Differences in the means between normal brain and stroke region for each parameter are all statistically significant (paired t test, $P < .01$).

Descriptive statistics (means and SDs) for spin density, T2, and ADC were computed, and differences in these parameters between the stroke region and normal brain were analyzed by means of a paired Student t test. As outlined in the Appendix, percentage changes in each tissue parameter as a function of infarct age were computed. These percentage changes in tissue parameters were also displayed graphically with simple linear or quadratic least squares regression lines added to assist visualization of trends as a function of time after infarction.

To understand the individual contributions of these changes in spin density, T2, and ADC to overall SI on DW images, these measured values were substituted one at a time into the model (22,23) for MR SI of the DW imaging sequence as shown in the Appendix. With this model, expected ratios of SI in the stroke region to normal brain resulting from differences in spin density, T2, and ADC could then be independently calculated and represented as SI enhancement ratios due to each parameter (spin density, T2, and ADC).

RESULTS

Each infarction imaged during the 1st week was noted to be markedly hyperintense to normal brain on DW images (Figs 1–3), with an average stroke-to-brain SI enhancement ratio (SIR_{total}) of 2.29. This increased total SI from stroke, also documented in multiple previous reports (6,17,21–23), is consistent with measured differences in spin density, T2, and ADC between stroke region and normal brain. On the average, we found that spin density and T2 increased by approximately 22% and 41%, respectively, whereas ADC values decreased by about 35% (Table 1).

Examination of the time course of these changes is even more enlightening. As seen in Figure 4a, the stroke-to-brain SI ratio on DW images remained relatively constant over the 1st week, decreasing only 1.5% per day (on the basis of the equation for the regression line). However, the relative values of spin density, T2, and ADC differed markedly as a function of time during this period (Table 2, Fig 4b–4d). Spin-density values became elevated above baseline by about 20% on day 1, with only a minimal further increase noted throughout the remainder of the 1st week. T2 values were elevated less than 20% in the first 2 days, but they rose to 70%–80% by the end of the 1st week. ADC values had a time course opposite that of T2 values, initially falling by approximately 60% but returning nearly to normal by the end of the 1st week.

The individual effects on total SI of these time-dependent changes in spin density, T2, and ADC can be analyzed by looking at their SI enhancement ratios (Fig 5). With our diffusion sequence with echo time of 97 msec and *b* value of 1,000 sec/mm^2, overall SI is dominated by diffusion effects for the first 2–3 days. Thereafter, T2 effects account for most of the high SI seen on the DW images. By day 7, almost all of the increased SI on DW images within the infarction was due to T2 effects, with only a modest contribution from spin-density effects.

DISCUSSION

DW MR imaging has become an important component of the modern imaging

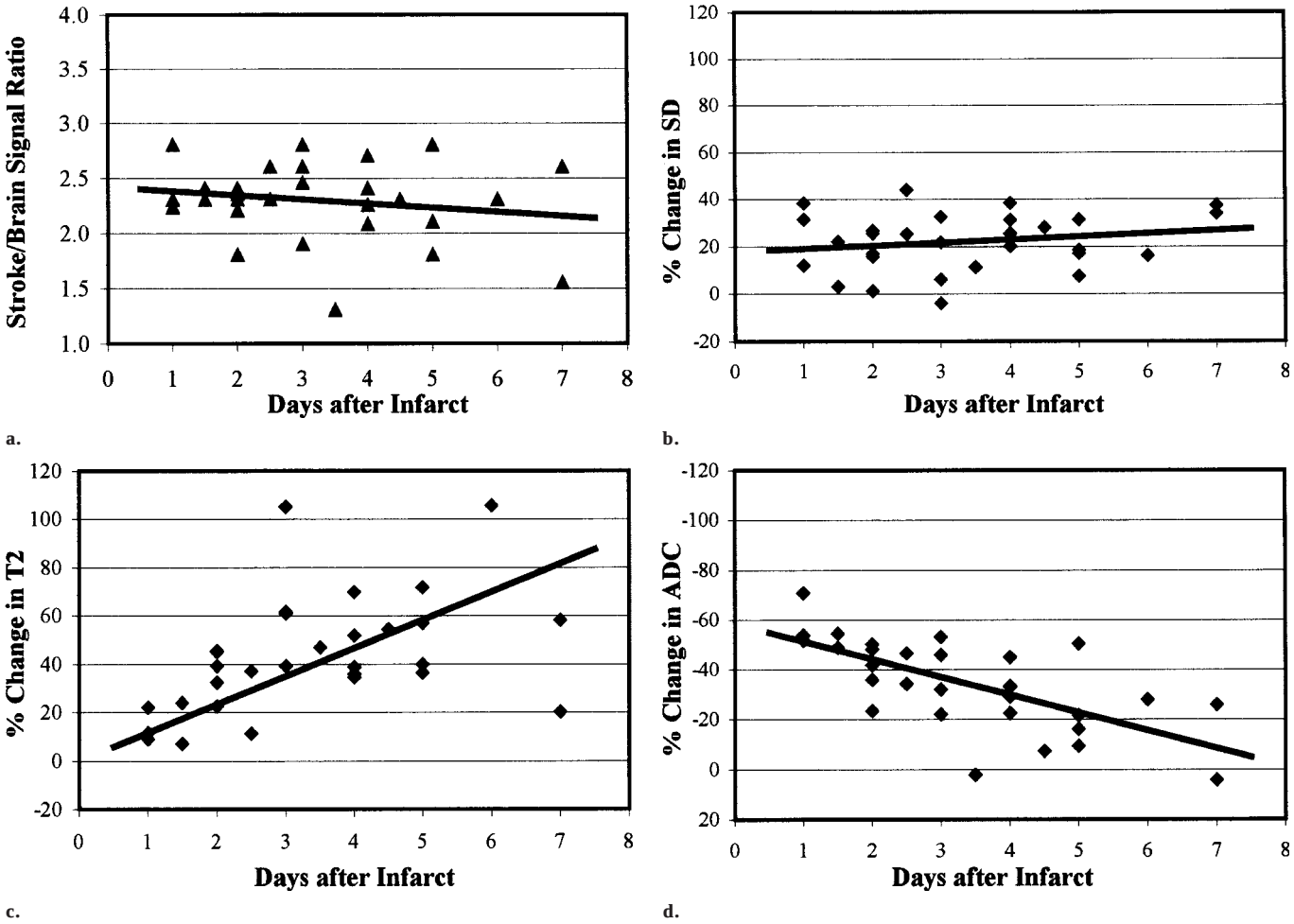

Figure 4. Changes in DW SI and tissue parameters as a function of time show the greatest initial change to be in ADC values and the greatest change by the end of the 1st week to be in T2 values. **(a)** Stroke-to-brain SI ratio is seen to remain relatively constant over the entire week. **(b)** Spin-density (*SD*) values remain elevated by approximately 20%–25% throughout the 1st week. **(c)** T2 values progressively increase over the 1st week. **(d)** ADC values are sharply reduced immediately after infarction, returning to nearly normal by the end of the week.

armamentarium for the diagnosis of acute cerebral infarction (1–18). In animal models, DW images can reliably reveal infarcted areas within minutes of experimental vascular occlusion (3,5,6). Although only a few clinical examples are available of human strokes imaged at such short time intervals, many positive DW images in patients with strokes only a few hours old have been published (8–14).

In addition to evaluating DW images, several investigators have used stepped gradient techniques to estimate changes in ADC after acute cerebral infarction. Reith et al (16) noted changes in ADC values within 5 minutes of onset of ischemia. Schlaug et al (17) found reduction, pseudonormalization, or even elevation of ADC values after the 7th day after infarction. Lutsep et al (11) found that ADC values remained low for the 1st week after infarction and normalized or became elevated at more chronic time points. Warach et al (8) and Marks et al (13) both found that after the initial decrease in the acute stroke period, ADC values gradually increased and became elevated after 10 days.

Although calculation of ADC values and production of ADC maps yields quantifiable results, it currently requires a level of data processing and complexity more extensive than is commonly available in most clinical MR centers. In current practice at most sites today, visual assessment of DW images (rather than ADC maps) is commonly employed for the diagnosis of stroke. The analogy is that even though it is possible to generate T1 and T2 maps from the MR raw data, this step is seldom performed. Radiologists prefer to use T1- or T2-weighted images for diagnosis, even though such images lack parameter "purity" and contain mixed contributions to overall SI (25).

As with T1- and T2-weighted images, DW images are not pure maps of ADC but contain mixed contributions from spin-density and T2 effects. We have referred to this phenomenon as MR shine through and have attempted to quantify its importance in clinical DW imaging. Other investigators have also recognized that shine-through effects exist in the DW imaging of stroke but have not thoroughly quantified them. Because of these shine-through effects, the DW images should be interpreted with reference to images obtained with other sequences, such as T2-weighted images, fluid-attenuated inversion-recovery, or FLAIR, images, and ADC maps (18).

Without actually calculating T2 values, Lutsep et al (11) noted a discrepancy in the temporal evolution of ADC and SI

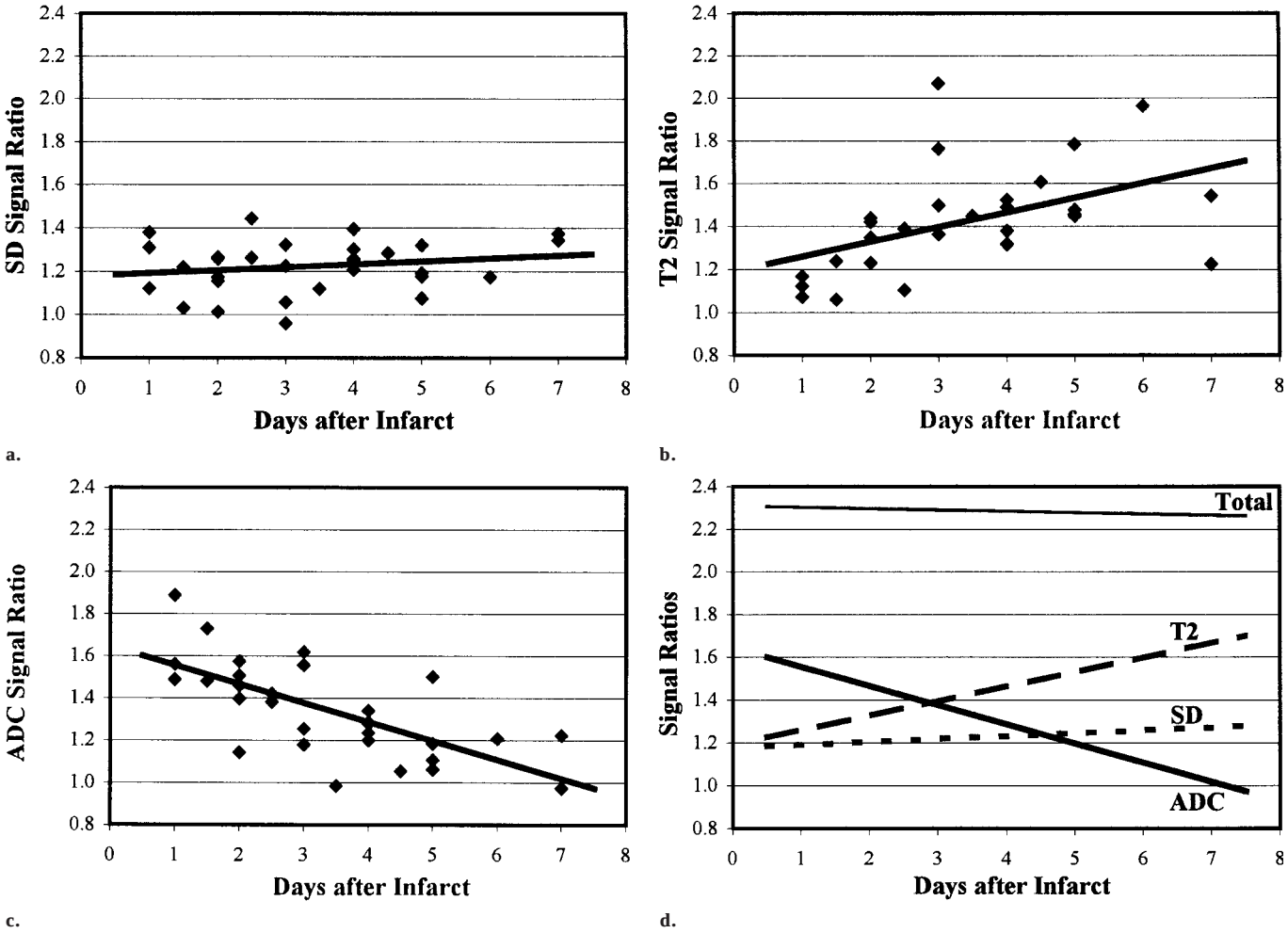

Figure 5. SI enhancement contributions to total DW SI by individual parameter and day. With our DW sequence, the overall SI is dominated by diffusion effects in the first 2–3 days; thereafter, T2 effects account for most of the high SI with only a modest contribution from spin-density (*SD*) effects. **(a)** Spin-density effects. **(b)** T2 effects. **(c)** ADC effects. **(d)** Individual contributions displayed together.

changes on T2-weighted images within 10 days after stroke (11). Burdette et al (14) noted the discrepancy in time course of SI changes of subacute cerebral infarction on T2-weighted and DW images; whereas ADC maps return to normal by 7–10 days, DW images may remain abnormal for up to 2 weeks. Knight et al (19) calculated ADC, T2, and T1 values in ischemic regions in rats after occlusion of the middle cerebral artery and found behavior of T1, T2, and spin density independent from that of ADC. They noted that the hyperintense appearance of infarcts on DW images cannot be attributed solely to ADC values and that care must be taken when SI abnormalities on DW images are interpreted.

By extending the work of these investigators, we quantified the independent contributions of ADC, T2, and spin density to the SI changes seen on DW images

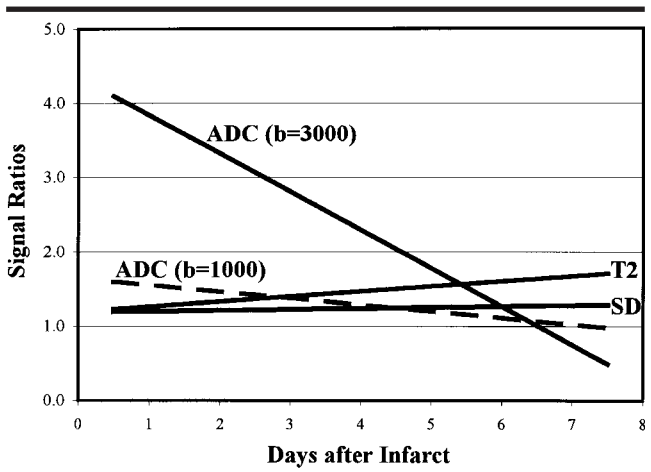

Figure 6. Theoretic individual contributions of ADC, T2, and spin density (*SD*) to DW image contrast for *b* values of 3,000 versus 1,000 sec/mm^2. The threefold increase in *b* value markedly increases the relative contribution of ADC to overall SI, but, by day 6, T2 and spin-density shine through still occur, eventually dominating the MR SI.

as a function of time during the 1st week after cerebral infarction. Our findings show that with use of current diffusion gradients with maximum *b* values of 1,000 sec/mm^2, all three components contribute to increased SI within the infarct on DW images. For the first 2–3 days, the increased SI on DW images results principally from restricted diffusion (ie, shortening of ADC). Thereafter, T2 effects, and to a lesser degree spin-density effects, provide the dominant mechanism of image contrast.

With advancing technology, stronger gradients will allow higher *b* values and consequently more ADC contrast to be present on DW images. The quantitative data in this report allow predictions of the degree of spin-density and T2 shine through that will be present on the next generation of diffusion-sensitive images. The SI enhancement ratio due to diffusion scales exponentially with *b* value (20). For example, each doubling of gradient *b* values squares the SI contribution of ADC to the DW image.

By using our model and data, it is possible to calculate the anticipated effect of increasing gradient strength on T2 shine through and the time course of total stroke SI on DW images. In Figure 6, we plotted the expected SI enhancement ratios of cerebral infarction for spin density, T2, and ADC in a high-performance gradient system with a *b* value of 3,000 sec/mm^2. As expected, this threefold increase in *b* value dramatically increased the relative contribution of ADC to the overall MR SI. By day 6, however, T2 and spin-density shine through still occurred, eventually dominating the MR SI.

In summary, with use of current gradient strengths with *b* values of 1,000 sec/mm^2, T2 (and to a lesser degree spin-density) shine-through effects account for a substantial component of the total MR SI observed on DW images of subacute cerebral infarction, especially beyond 3–4 days. The future use of gradients with higher strength will shift the timing of this effect but will not eliminate it.

TABLE 2
Changes in Spin Density, T2, and ADC due to Infarction

Case No.	Time after Infarct (day)	Percentage Change in Spin Density	Percentage Change in T2	Percentage Change in ADC
1	1.0	12	9	−71
2	1.0	38	11	−54
3	1.0	31	22	−52
4	1.5	22	24	−49
5	1.5	3	7	−55
6	2.0	26	32	−48
7	2.0	16	23	−50
8	2.0	1	46	−23
9	2.0	17	39	−42
10	2.0	27	45	−36
11	2.5	44	11	−34
12	2.5	25	37	−47
13	3.0	33	39	−46
14	3.0	6	61	−53
15	3.0	22	62	−22
16	3.0	−4	105	−32
17	3.5	11	47	+2
18	4.0	38	36	−33
19	4.0	25	52	−23
20	4.0	26	70	−45
21	4.0	20	35	−34
22	4.0	31	39	−29
23	4.5	28	54	−7
24	5.0	17	72	−16
25	5.0	8	40	−9
26	5.0	31	37	−22
27	5.0	19	57	−28
28	6.0	16	106	−28
29	7.0	38	58	−26
30	7.0	34	20	+4

APPENDIX

The percentage changes in each tissue parameter (*P*) as a function of infarct age were computed with the following formula:

$$\%\Delta P = \frac{P_{\text{Stroke}} - P_{\text{Normal}}}{P_{\text{Normal}}} \times 100$$

where *P* is spin density, T2, or ADC, respectively. These percentage changes in tissue parameters were also displayed graphically, with simple linear or quadratic least squares regression lines added to assist visualization of trends as a function of time after infarction.

To understand the individual contributions of these changes in spin density (SD), T2, and ADC to overall SI on DW images, these measured values were substituted one at a time into the following model (22,23) for MR SI of the DW imaging sequence:

$$\text{SI} = k \cdot \text{SD} \cdot e^{-\text{TE/T2}} \cdot e^{-b \cdot \text{ADC}}.$$

For our experiments, *k* is an arbitrary scaling constant, echo time (TE) is 97 msec, and the *b* value is 1,000 sec/mm^2. Note that because we used a single-shot, echo-planar diffusion technique, the repetition time is effectively infinite, and T1 effects make no significant contributions to the MR SI.

By using this model, expected ratios of SI in the stroke region to normal brain resulting from differences in spin density, T2, and ADC could then be independently calculated. For example, we defined the SI enhancement ratio (SIR) due to T2 effects alone (SIR_{T2}) in stroke region (S) relative to normal (N) brain as

$$\text{SIR}_{\text{T2}} = \frac{k \cdot \text{SD}_\text{N} \cdot e^{-\text{TE/T2}_\text{S}} \cdot e^{-b \cdot \text{ADC}_\text{N}}}{k \cdot \text{SD}_\text{N} \cdot e^{-\text{TE/T2}_\text{N}} \cdot e^{-b \cdot \text{ADC}_\text{N}}} = \frac{e^{-\text{TE/T2}_\text{S}}}{e^{-\text{TE/T2}_\text{N}}}.$$

Similarly, the SI enhancement ratios due to spin-density effects alone (SIR_{SD}) and ADC effects alone (SIR_{ADC}) were defined as

$$\text{SIR}_{\text{SD}} = \frac{\text{SD}_\text{S}}{\text{SD}_\text{N}} \quad \text{and} \quad \text{SIR}_{\text{ADC}} = \frac{e^{-b \cdot \text{ADC}_\text{S}}}{e^{-b \cdot \text{ADC}_\text{N}}}.$$

Note that the total SI enhancement ratio of stroke to normal brain with the DW pulse sequence ($\text{SIR}_{\text{total}}$) is merely the product of the individual enhancement ratios:

$$\text{SIR}_{\text{TOT}} = \frac{\text{SI}_\text{S}}{\text{SI}_\text{N}} = \text{SIR}_{\text{SD}} \cdot \text{SIR}_{\text{T2}} \cdot \text{SIR}_{\text{ADC}}.$$

This formulation provided a useful check on individual SI enhancement ratio calculations and on the overall consistency of our results.

Acknowledgments: The authors thank Hugh Howards, PhD, for help with the statistical analysis, Shona Simpson, PhD, for editorial comments, and the MR imaging technologists for their patience and support for clinical MR imaging research.

References

1. Kucharczyk J, Mintorovitch J, Asgari HS, Moseley M. Diffusion/perfusion MR imaging of acute cerebral ischemia. Magn Reson Med 1991; 19:311–315.
2. Jones SC, Perez-Trepichio AD, Xue M, Furlan AJ, Awad IA. Magnetic resonance diffusion-weighted imaging: sensitivity and apparent diffusion constant in stroke. Acta Neurochir Suppl (Wien) 1994; 60: 207–210.
3. Minematsu K, Li L, Sotak CH, Davis MA, Fisher M. Reversible focal ischemic injury demonstrated by diffusion-weighted magnetic resonance imaging in rats. Stroke 1992; 23:1304–1311.
4. Moseley ME, Kucharczyk J, Mintorovitch J, et al. Diffusion-weighted MR imaging of acute stroke: correlation with T2-weighted and magnetic susceptibility–enhanced MR imaging in cats. AJNR 1990; 11:423–429.
5. Moseley ME, Cohen Y, Mintorovitch J, et al. Early detection of regional cerebral ischemia in cats: comparison of diffusion- and T2-weighted MRI and spectroscopy. Magn Reson Med 1990; 14:330–346.
6. Mintorovitch J, Moseley ME, Chileuitt L, Shimizu H, Cohen Y, Weinstein PR. Comparison of diffusion- and T2-weighted MRI for the early detection of cerebral ischemia and reperfusion in rats. Magn Reson Med 1991; 18:39–50.
7. Moonen CT, Pekar J, de Vleeschouwer MH, van Gelderen P, van Zijl PC, DesPres D. Restricted and anisotropic displacement of water in healthy cat brain and in stroke studied by NMR diffusion imaging. Magn Reson Med 1991; 19:327–332.
8. Warach S, Gaa J, Siewert B, Wielopolski P, Edelman RR. Acute human stroke studied by whole brain echo planar diffusion-weighted magnetic resonance imaging. Ann Neurol 1995; 37:231–241.
9. Warach S, Dashe JF, Edelman RR. Clinical outcome in ischemic stroke predicted by early diffusion-weighted and perfusion magnetic resonance imaging: a preliminary analysis. J Cereb Blood Flow Metab 1996; 16:53–59.
10. Sorensen AG, Buonanno FS, Gonzalez RG, et al. Hyperacute stroke: evaluation with combined multisection diffusion-weighted and hemodynamically weighted echo-planar MR imaging. Radiology 1996; 199:391–401.
11. Lutsep HL, Albers GW, DeCrespigny A, Kamat GN, Marks MP, Moseley ME. Clinical utility of diffusion-weighted magnetic resonance imaging in the assessment of ischemic stroke. Ann Neurol 1997; 41: 574–580.
12. Warach S, Chien D, Li W, Ronthal M, Edelman RR. Fast magnetic resonance diffusion-weighted imaging of acute human stroke. Neurology 1992; 42:1717–1723.
13. Marks MP, de Crespigny A, Lentz D, Enzmann DR, Albers GW, Moseley ME. Acute and chronic stroke: navigated spin-echo diffusion-weighted MR imaging. Radiology 1996; 199:403–408.
14. Burdette JB, Ricci PE, Petitti N, Elster AD. Cerebral infarction: time course of signal changes on diffusion-weighted MR images. AJR 1998; 171:791–795.
15. Le Bihan D, Breton E, Lallemand D, Grenier P, Cabanis E, Laval-Jeantet M. MR imaging of intravoxel incoherent motions: application to diffusion and perfusion in neurologic disorders. Radiology 1986; 161:401–407.
16. Reith W, Hasegawa Y, Latour LL, Dardzinski BJ, Sotak CH, Fisher M. Multislice diffusion mapping for 3-D evolution of cerebral ischemia in a rat stroke model. Neurology 1995; 45:172–177.
17. Schlaug G, Siewert B, Benfield A, Edelman RR, Warach S. Time course of the apparent diffusion coefficient (ADC) abnormalities in human stroke. Neurology 1997; 49:113–119.
18. Beauchamp NJ, Bryan RN. Acute cerebral ischemic infarction: a pathophysiologic review and radiologic perspective. AJR 1998; 171:73–84.
19. Knight RA, Dereski MO, Helpern JA, Ordidge RJ, Chopp M. Magnetic resonance imaging assessment of evolving focal cerebral ischemia: comparison with histopathology in rats. Stroke 1994; 25:1252–1262.
20. Stejskal EO, Tanner JE. Spin diffusion measurements: spin echoes in the presence of a time-dependent field gradient. J Chem Phys 1965; 42:288–292.
21. Burdette JH, Elster AD, Ricci PE. Calculation of apparent diffusion coefficients (ADCs) in brain using two-point and six-point methods. J Comput Assist Tomogr 1998; 22:792–794.
22. Xing D, Papadakis NG, Huang CL, Lee VM, Carpenter TA, Hall LD. Optimized diffusion-weighting for measurement of apparent diffusion coefficient (ADC) in human brain. Magn Reson Imaging 1997; 15:771–784.
23. Kjos BO, Ehman RL, Brant-Zawadski M, Kelly WM, Norman D, Newton TH. Reproducibility of relaxation times and spin density calculated from routine MR imaging sequences: clinical study of the CNS. AJR 1985; 144:1165–1170.
24. Breger RK. Reproducibility of relaxation and spin-density parameters in phantoms and the human brain measured by MR imaging at 1.5 T. Magn Reson Med 1986; 3:649–662.
25. Elster AD. An index system for comparative parameter weighting in MR imaging. J Comput Assist Tomogr 1988; 12:130–134.